Investigating causal biological relationships between reproductive performance traits in high-performing gilts and sows[1]

Kessinee Chitakasempornkul,* Mariana B. Meneget,† Guilherme J. M. Rosa,‡ Fernando B. Lopes,‡ Abigail Jager,* Márcio A. D. Gonçalves,§ Steve S. Dritz,†,◉ Mike D. Tokach,# Robert D. Goodband,# and Nora M. Bello*,2,◉

*Department of Statistics, Kansas State University, Manhattan 66506, KS; †Department of Diagnostic Medicine/Pathobiology, Kansas State University, Manhattan 66506, KS; ‡Department of Animal Sciences, University of Wisconsin-Madison, Madison 53706, WI; §Jefo Nutrition, Saint-Hyacinthe, QC J2R 2E7, Canada; and #Department of Animal Sciences and Industry, Kansas State University, Manhattan 66506, KS

ABSTRACT: Efficient management of swine production systems requires understanding of complex reproductive physiological mechanisms. Our objective in this study was to investigate potential causal biological relationships between reproductive performance traits in high-producing gilts and sows. Data originated from a nutrition experiment and consisted of 200 sows and 440 gilts arranged in body weight blocks and randomly assigned to dietary treatments during late gestation at a commercial swine farm. Reproductive performance traits consisted of weight gain during late gestation, total number born and number born alive in a litter, born alive average birth weight, wean-to-estrous interval, and total litter size born in the subsequent farrowing. Structural equation models combined with the inductive causation algorithm, both adapted to a hierarchical Bayesian framework, were employed to search for, estimate, and infer upon causal links between the traits within each parity group. Results indicated potentially distinct reproductive networks for gilts and for sows. Sows showed sparse connectivity between reproductive traits, whereas the network learned for gilts was densely interconnected, suggesting closely linked physiological mechanisms in younger females, with a potential for ripple effects throughout their productive lifecycle in response to early implementation of tailored managerial interventions. Cross-validation analyses indicated substantial network stability both for the general structure and for individual links, though results about directionality of such links were unstable in this study and will need further investigation. An assessment of relative statistical power in sows and gilts indicated that the observed network discrepancies may be partially explained on a biological basis. In summary, our results suggest distinctly heterogeneous mechanistic networks of reproductive physiology for gilts and sows, consistent with physiological differences between the groups. These findings have potential practical implications for integrated understanding and differential management of gilts and sows to enhance efficiency of swine production systems.

Key words: hierarchical Bayesian models, structural equation model, structure learning, swine reproductive physiology

INTRODUCTION

Female reproductive physiology involves complex mechanisms that need to be integrated and managed efficiently in swine production systems. Understanding the functional links that underlie the relationship between multiple reproductive performance traits can provide valuable mechanistic insight, and thus enhance efficiency of the decision-making process in swine production systems. Classical multiple-trait models (**MTM**s) can be used to simultaneously consider multiple traits and study their probabilistic relationships, expressed as correlations or covariances (Henderson and Quaas, 1976; Van Vleck and Edlin, 1984). However, classical MTMs are limited in that they cannot assess directionality of such relationships (Valente and Rosa, 2013), thus hindering their use for exploring causal relationships within a network, as might be of interest in complex systems with multiple interrelated traits.

Structural equation models (**SEM**s) (Haavelmo, 1943) are a special type of MTM that, under some assumptions, can accommodate directionality and thus potentially causal relationships in the links that define a functional network (Pearl, 2009). Thus, an SEM approach can facilitate a more comprehensive understanding of physiological mechanisms as an interconnected system, as opposed to an assortment of individual outcome traits, the relationship among which is evaluated only anecdotally or, at best, one at a time. Originally evolved from path analysis (Wright, 1934), SEMs were recently adapted to a mixed-model framework (Gianola and Sorensen, 2004), thereby enabling specification of data architecture, as is typically the case with designed experiments. Search algorithms, such as inductive causation (**IC**; Verma and Pearl, 1991), are also available to help investigate the network space while accounting for multiple levels of data structure (Valente et al., 2010). Given these developments, SEM are being increasingly used in the animal sciences, particularly in quantitative genetics. Examples include beef cattle (Inoue et al., 2016), dairy cattle (de Maturana et al., 2009), dairy goats (de los Campos et al., 2006), swine (Varona and Sorensen, 2014), and quail (Valente et al., 2011), among others.

Here, our interest in causal network-type relationships is motivated by a recent swine experiment conducted to evaluate the effect of nutritional management during late gestation on multiple reproductive performance traits in high-performing gilts and sows (Gonçalves et al., 2016). In that experimental study, each trait was analyzed separately using a generalized linear mixed-model approach, whereby each trait represented related, though arguably different, aspects of swine reproductive physiology. The randomization process in that experiment granted causal inference of nutritional dietary treatment on each individual trait. In the study herein, we pursue a more comprehensive understanding of the reproductive physiological system as a whole, recognizing that, in addition to treatment effects, reproductive performance traits may also influence each other within the system.

The objective of this study was to investigate potential causal biological relationships between reproductive performance traits in high-producing gilts and sows in the context of a designed nutrition experiment. Using hierarchical SEM combined with IC, we search for, estimate, and infer upon potential causal network-type interrelationships between reproductive traits in sows and gilts. We further evaluate the stability of the learned network structures and assess potential differences in statistical power between the parity groups.

MATERIALS AND METHODS

Data

Data were obtained from an experimental study on swine nutrition conducted at a commercial swine farm in northern Ohio under an experimental protocol approved by the Kansas State University Institutional Animal Care and Use Committee, as described by Gonçalves et al. (2016). The complete experimental data consisted of observations from 1,102 females, including 361 sows and 741 gilts. For each parity group (i.e., sows and gilts), the experimental design used for data collection consisted of a randomized complete block design with blocks of 4 females defined along a body weight gradient. Within each block, 4 dietary treatments consisting of combinations of energy intake and dietary amino acids were randomly allocated. The complete description of the data is available in Gonçalves et al. (2016). The reproductive performance traits of interest, labeled $j = 1,\ldots, J$, for $J = 6$, included female weight gain during late (day 90 to day 111) gestation (**GAIN**, in kilograms; $j = 1$), total number of piglets born (**TB**; $j = 2$) and number born alive (**BA**; $j = 3$) in a litter, and born alive average birth weight (**BABW**, in grams; $j = 4$), wean-to-estrous interval (**WEI**, in days; $j = 5$), and total litter size born in the subsequent farrowing (**SuTB**; $j = 6$). Observations on GAIN were obtained as the difference in female body weight observed at day 90

and at day 111 of gestation. Observations on TB, BA, and BABW were collected simultaneously at the time of farrowing and preceded those observations on WEI, which in turn preceded data collection on SuTB. Both TB and SuTB refer to total litter size and included piglets born alive, stillborns, and mummies. Only females with complete records on all 6 reproductive performance traits (i.e., no missing data) were considered for analyses in this study. Following data editing for removal of incomplete records, the final dataset used for analysis consisted of 200 sows and 440 gilts arranged in 97 and 222 body weight blocks, respectively. As a result, the dataset analyzed consisted of incomplete blocks that ranged in size from 1 to 4 females.

The Structural Equation Model

For each parity group, namely sows and gilts, we write a hierarchical SEM following Gianola and Sorensen (2004), as follows:

$$y_i = \Lambda y_i + X_i \beta + Z_i b + e_i \quad (1)$$

where $y'_i = [y_{i1}, y_{i2}\ y_{i3}\ y_{i4}\ y_{i5}\ y_{i6}]$ i++s a vector of $J = 6$ reproductive performance traits observed on the ith female ($i = 1, 2, …, n$; corresponding to $n = 200$ sows or $n = 440$ gilts, respectively). Also, Λ is a $J \times J$ matrix composed by zeroes along the main diagonal and on the upper triangle, and unknown structural coefficient parameters $\lambda_{jj'}$ on the lower triangle (under a fully recursive specification) representing functional links between responses in the network. The structural coefficient $\lambda_{jj'}$ ($j' < j$) describes the direct effect of trait $y_{j'}$ on trait y_j. For example, λ_{21} represents the expected change in y_2 per unit increase in y_1. Further, $\beta' = [\beta'_1\ \beta'_2\ \beta'_3\ \beta'_4\ \beta'_5\ \beta'_6]$ is a vector of unknown fixed-effect location parameters associated with treatment factors through the design matrix $X_i = diag(x'_{i1}\ x'_{i2}\ x'_{i3}\ x'_{i4}\ x'_{i5}\ x'_{i6})$ unique to each subject i. Next, $b' = [b'_1\ b'_2\ b'_3\ b'_4\ b'_5\ b'_6]$ is a vector of unknown random effects associated with body weight blocks expressed in the design matrix $Z_i = diag(z'_{i1}\ z'_{i2}\ z'_{i3}\ z'_{i4}\ z'_{i5}\ z'_{i6})$. Random effects b are assumed multivariate normally distributed with null mean vector and covariance matrix B, such that:

$$b \sim MVN\left(0, B \otimes I_q = \begin{bmatrix} \sigma^2_{b_1} & \sigma_{b_{12}} & \sigma_{b_{13}} & \sigma_{b_{14}} & \sigma_{b_{15}} & \sigma_{b_{16}} \\ \sigma_{b_{12}} & \sigma^2_{b_2} & \sigma_{b_{23}} & \sigma_{b_{24}} & \sigma_{b_{25}} & \sigma_{b_{26}} \\ \sigma_{b_{13}} & \sigma_{b_{23}} & \sigma^2_{b_3} & \sigma_{b_{34}} & \sigma_{b_{35}} & \sigma_{b_{36}} \\ \sigma_{b_{14}} & \sigma_{b_{24}} & \sigma_{b_{34}} & \sigma^2_{b_4} & \sigma_{b_{45}} & \sigma_{b_{46}} \\ \sigma_{b_{15}} & \sigma_{b_{25}} & \sigma_{b_{35}} & \sigma_{b_{45}} & \sigma^2_{b_5} & \sigma_{b_{56}} \\ \sigma_{b_{16}} & \sigma_{b_{26}} & \sigma_{b_{36}} & \sigma_{b_{46}} & \sigma_{b_{56}} & \sigma^2_{b_6} \end{bmatrix} \otimes I_q\right) \quad (2)$$

where q is the number of blocks within each parity group. Finally, $e'_i = [e_{i1}\ e_{i2}\ e_{i3}\ e_{i4}\ e_{i5}\ e_{i6}]$ is the corresponding set of residuals for the ith female, assumed multivariate normally distributed with null mean vector and diagonal (co)variance matrix R, such that:

$$e_i \sim MVN\left(0, R = \begin{bmatrix} \sigma^2_{e_1} & 0 & 0 & 0 & 0 & 0 \\ 0 & \sigma^2_{e_2} & 0 & 0 & 0 & 0 \\ 0 & 0 & \sigma^2_{e_3} & 0 & 0 & 0 \\ 0 & 0 & 0 & \sigma^2_{e_4} & 0 & 0 \\ 0 & 0 & 0 & 0 & \sigma^2_{e_5} & 0 \\ 0 & 0 & 0 & 0 & 0 & \sigma^2_{e_6} \end{bmatrix}\right) \quad (3)$$

The assumption of a diagonal residual (co)variance matrix R is standard in the context of SEM to ensure parameter identifiability in an acyclic causal framework (Gianola and Sorensen, 2004). Any additional source of covariability (besides random effects) is attributed to structural coefficients in Λ and refers to functional relationships between traits (Gianola and Sorensen, 2004; Wu et al., 2007).

The IC Algorithm

We implemented the IC algorithm as adapted to mixed models by Valente et al. (2010) to search the space of network structures separately for each parity group. The search was conducted at the residual level of a MTM, that is, after conditioning on the random effects that characterize the experimental design. This approach prevents the structure search from being confounded by correlations between traits that might be induced by the design structure of the data; this is analogous to the approach proposed by Valente et al. (2010) in the context of quantitative genetics. Briefly, we first fit a hierarchical Bayesian SEM with a fully recursive specification equivalent to a standard MTM to the data. Posterior samples of the SEM parameters in matrices R and Λ were used to compute the posterior densities for parameters of R^* defined as the residual (co)variance matrix under the equivalent MTM, whereby $R^* = (I - \Lambda)^{-1} R(I - \Lambda)^{-1'}$. Next, we used posterior samples of R^* to compute partial residual correlations for each pair of reproductive performance traits, given all possible conditioning sets consisting of combinations of the remaining traits. Finally, we implemented the IC algorithm on such partial residual correlations between traits to make a series of statistical decisions intended to yield a learned network structure (Valente et al., 2010), as follows:

Step 1: For each pair of traits y_j and $y_{j'}$, evaluate all partial residual correlations conditional on every possible conditioning set of traits besides the (j, j') pair. If all such partial correlations differ from zero, connect the traits by an undirected link (e.g., $y_j \longrightarrow y_{j'}$). Otherwise, no connecting link is placed between the traits in that pair. After considering all pairs of traits, this step yields an undirected (skeleton) graph.

Step 2: From the skeleton obtained in Step 1, consider every pair of disconnected traits that share a common adjacent trait (e.g. y_j and $y_{j''}$ in $y_j \longrightarrow y_{j'} \longrightarrow y_{j''}$) and evaluate all partial residual correlations between the pair that include the common adjacent trait ($y_{j'}$) in the conditioning set. If all such conditional partial correlations differ from zero, direct the edges towards the common adjacent trait (i.e., $y_j \rightarrow y_{j'} \leftarrow y_{j''}$); this identifies a network structure known as an unshielded collider. This step yields a partially directed graph (Pearl, 2009).

Step 3: Based on the partially directed graph obtained from Step 2, orient as many undirected edges as possible without creating any new unshielded colliders nor any cycles. Graphs obtained in Step 3 represent a class of equivalent causal structures (i.e., structures that would result in the same space of joint probability distributions) (Pearl, 2009). In a hierarchical modeling context, the IC algorithm is implemented on the residual (co)variance matrix $\boldsymbol{R}^*$ (Valente et al., 2010), such that equivalence classes are defined in the space of residual joint probability distributions.

The inferential basis for each of the statistical decisions made in Steps 1 and 2 of the IC algorithm was the highest posterior density (HPD) interval of the partial residual correlations between traits and whether such intervals contained the value zero. We applied different probability contents of the HPD interval, namely 70%, 75%, 80%, 85%, 90%, and 95%, to learn the causal structures. Supplementary Figures 1–3 show the network structures recovered for sows (gilts) across the range of evaluated probability contents of HPD intervals. For sows, when 85%, 90%, and 95% HPD intervals were applied, no links between any of the reproductive traits were recovered; an 80% HPD interval was the highest probability content that recovered links in the network structure. For gilts, IC Steps 1 and 2

using 95%, 90%, and 85% HPD intervals detected links between some of the reproductive traits (Supplementary Figure 2), though GAIN remained disconnected in all cases. An 80% HPD interval was the largest probability content that connected all traits in the gilt dataset (Supplementary Figure 3). For consistency of reporting, we chose to proceed with 80% HPD intervals for both sows and gilts in an attempt to balance the probability of missing true connections (Type II error) with the probability of including false ones (Type I error). This is consistent with previous applications (Inoue et al., 2016).

After Step 3 of the IC algorithm, we used additional information to direct any left-over undirected edges, including temporal arrangement of traits and model fit comparisons based on Deviance Information Criterion (**DIC**) (Spiegelhalter et al., 2002). Models that better fit the data are characterized by smaller DIC values, and generally differences of 7 or greater are considered indicative of improved model fit (Spiegelhalter et al., 2002).

Hierarchical Bayesian Implementation and Posterior Inference

The selected SEM specification was fit in a hierarchical Bayesian framework implemented with Markov chain Monte Carlo (**MCMC**). The joint posterior distribution of all unknown parameters in the model was:

$$p(\boldsymbol{\beta}, \boldsymbol{b}, \boldsymbol{B}, \boldsymbol{R}, \boldsymbol{\Lambda} | \boldsymbol{y}) \propto p(\boldsymbol{y} \mid \boldsymbol{\beta}, \boldsymbol{b}, \boldsymbol{R}, \boldsymbol{\Lambda}) \, p(\boldsymbol{\beta})$$
$$p(\boldsymbol{b} \mid \boldsymbol{B}) \, p(\boldsymbol{B}) \, p(\boldsymbol{R}) \, p(\boldsymbol{\Lambda})$$

$$(4)$$

We used conditionally conjugate prior distributions to facilitate Gibbs sampling. Prior distributions for fixed-effects location parameters $\boldsymbol{\beta}_j$ and each of the non-zero structural coefficients $\lambda_{jj'}$ in matrix $\boldsymbol{\Lambda}$ were assumed flat such that $p(\boldsymbol{\beta}_j) \propto$ constant and $p(\lambda_{jj'}) \propto$ constant for all j and j'. For each residual variance $\sigma_{e_j}^2$ along the main diagonal of $\boldsymbol{R}$, we generated a proxy for a flat, improper prior using as an instrument the density of a scale-inverse chi-square distribution and setting degrees of freedom $v_{e_j} = -1$ and scale parameter $s_{e_j}^2 = 0$. This proxy is consistent with the prior $\sqrt{\sigma_{e_j}^2} \sim U(0, A)$, for any finite but sufficiently large value of A, such that the resulting distribution is vague, as recommended for variance components by Gelman (2006). For the block effects $\boldsymbol{b}$, we specified a structural prior such that $p(\boldsymbol{b}|\boldsymbol{B}) \sim N(\boldsymbol{0}, \boldsymbol{B})$ to allow for borrowing of information across traits within each block (i.e., block

level covariance parameters), and also across body weight blocks for each trait (i.e., block level variance parameters) (Robinson, 1991), as is common for random effects in a multivariate mixed-model framework. For the (co)variance matrix $\boldsymbol{B}$, we implemented a proxy for a vague prior using as an instrument the density of an inverse-Wishart distribution, setting degrees of freedom $\nu_B = -(J + 1)$ and specifying a $J \times J$ scale matrix of zeroes; this can be interpreted as a multivariate extension of the proxy used for prior specification on the residual variances.

All MCMC implementations were programmed in R software (R Development Core Team, 2017). For each parity group, the fully recursive SEM of Eq. (1) was fit using a single MCMC chain run for 100,000 iterations after a burn-in period of 10,000 cycles; one of every 3 samples were saved and fed into the IC algorithm for structure search, as explained in the previous section. For final inference, the selected SEM with a specification of causal structure determined by the IC algorithm was fit using a single MCMC chain run for 300,000 iterations for a burn-in period of 10,000 cycles; one of every 3 samples were saved for inference. In all cases, convergence diagnostics were performed using the R package CODA (Cowles and Carlin, 1996). Specifically, we monitored convergence for all hyperparameters using trace plots and the diagnostic testing approach proposed by Raftery and Lewis (1992). Furthermore, effective sample size (**ESS**) was estimated to evaluate the number of effectively independent samples amongst the autocorrelated MCMC samples for each hyperparameter (Sorensen et al., 1995). Length of MCMC chains was adjusted to ensure that ESS was greater than 800 for all hyperparameters. For each parameter of interest, we summarized posterior inference using posterior means and 95% HPD intervals.

Assessment of Network Stability

For each parity group, we evaluated the stability of the learned networks using a Jackknife resampling approach adapted from Peñagaricano et al. (2015) for implementation to a network learning context. More specifically, we modified the resampling strategy to leave-one-*block*-out of the dataset at a time (as opposed to leave-one-*observation*-out). In each resampling iteration, the network structure was inferred from a new dataset by implementation of the IC algorithm on a fully recursive SEM specification based on 80% HPD

intervals, as described in the previous section. We evaluated the stability of each individual link by assessing the frequency of presence or absence, as well as direction, in the networks learned from the new datasets obtained from resampling.

Power Assessment in Network Learning

Recall that the size and structure of the datasets available for gilts (i.e., 440 females; 222 blocks) was approximately twice of that available for sows (i.e., 200 females; 97 blocks). Thus, it was of interest to assess whether any discrepancies in network learning might be due, at least partially, to differential power in the statistical decisions made to infer network structure. To evaluate this, we constructed 5 subsets of the gilt dataset by sampling it at random and without replacement; each gilt data subset mimicked the structure of the sow dataset in number of observations and number of blocks. For each gilt data subset, we learned network structure by implementing the mixed-model-adapted IC algorithm (Valente et al., 2011) as described in previous sections. We then compared the networks learnt from the gilt data subsets with those learnt from the complete datasets for gilts and for sows.

RESULTS

Descriptive Data Analyses

Descriptive statistics of the reproductive performance traits are presented separately for sows and gilts in Table 1. Also, for each parity group, the empirical distribution of each trait is presented on the main diagonal of Fig. 1, along with pairwise scatterplots and empirical marginal Pearson correlations in the lower and upper triangles of the figure, respectively. Except for WEI, reproductive performance traits showed approximately symmetrical empirical distributions, thereby supporting a normal approximation for modeling. By contrast, the empirical distribution of WEI was skewed to the right for both parity groups.

Pairwise scatterplots and marginal correlations described general similarities for both gilts and sows in the pairwise relationships between traits (Fig. 1), except for a few distinct patterns. For example, GAIN was positively correlated to TB, BA, and BABW in both parity groups but the numerical magnitude of the correlation coefficient appeared to be at least doubled in sows relative to gilts. Furthermore, the marginal Pearson correlation coefficient between WEI and SuTB was significantly

Table 1. Descriptive statistics of reproductive performance traits in sows and gilts

Trait[1]	Sows (n = 200)						Gilts (n = 440)					
	Mean	Min	25th percentile	Median	75th percentile	Max	Mean	Min	25th percentile	Median	75th percentile	Max
GAIN, kg	16.0	−1.8	11.2	15.4	20.9	36.3	17.9	−12.3	14.1	17.7	22.0	41.3
TB	15.4	6.0	14.0	15.0	17.0	21.0	14.3	6.0	13.0	14.0	16.0	21.0
BA	14.3	5.0	13.0	14.5	16.0	20.0	13.5	5.0	12.0	14.0	15.0	20.0
BABW, g	1,404	1,018	1,251	1,520	1,520	2,018	1,279	817	1,163	1,267	1,392	1,960
WEI, day	4.3	3.0	4.0	4.6	5.0	10.0	6.2	2.0	4.0	4.0	5.0	31.0
SuTB	14.9	2.0	13.0	15.0	17.0	24.0	13.2	1.0	11.0	14.0	16.0	25.0

[1]GAIN = female weight gain during late gestation; TB = total number born in a litter; BA = number born alive in a litter; BABW = born alive average body weight; WEI = wean-to-estrous interval; SuTB = total number born in the subsequent gestation.

different from zero for both groups, though of positive sign for gilts, and negative sign for sows. Overall, preliminary descriptive analyses suggested potential differences between gilts and sows in the network of interconnected reproductive traits. This finding motivated separate network analyses for each parity group.

Learned Network Structures Using the IC Algorithm

For each parity group, network structure was learned separately using the IC algorithm. Based on statistical decisions made on 80% HPD intervals, the network recovered for sows included links only among TB, BA, and BABW, whereas GAIN, WEI, and SuTB remained unconnected. Moreover, the IC algorithm did not resolve directionality for any of the links connecting TB, BA, and BABW in sows, thus yielding an undirected graph (Fig. 2A). It was not possible to further orient the links between BABW, BA, and TB based on temporal information because, in this study, these traits were realized simultaneously at farrowing. Therefore, for sows, we considered alternative SEMs connecting BABW, BA, and TB (Fig. 2B) that did not introduce any new unshielded colliders (which would presumably have been detected in Step 2 of the IC algorithm) and compared them for fit to data using DIC. Figure 2B shows competing SEM alternatives for sows, of which network (3) (i.e., BABW → BA → TB) was selected for further inference based on a DIC value smaller by 20 and 38 points from that of directed networks (1) or (2), respectively.

For gilts, Steps 1 and 2 of the IC algorithm yielded a partially oriented graph depicting an interconnected network that linked all 6 reproductive performance traits (Fig. 3A). Of special interest was the link between GAIN and BABW, the detection of which was pivotal to assess directionality in the gilt network because this link formed an unshielded collider with BA (i.e., GAIN → BABW ← BA). So directed, the link GAIN → BABW supported directionality for other links by negating unshielded colliders with TB (i.e., GAIN → BABW → TB) as well as with traits indicative of longer-term reproductive performance, namely WEI (i.e., GAIN → BABW → WEI) and SuTB (i.e., GAIN → BABW → SuTB). These results further oriented the remaining link connecting BA and TB as BA → TB to prevent formation of a cycle, as dictated by the IC algorithm. Overall, the IC algorithm applied to the gilt dataset concluded on an effect of GAIN on BABW (i.e., GAIN →
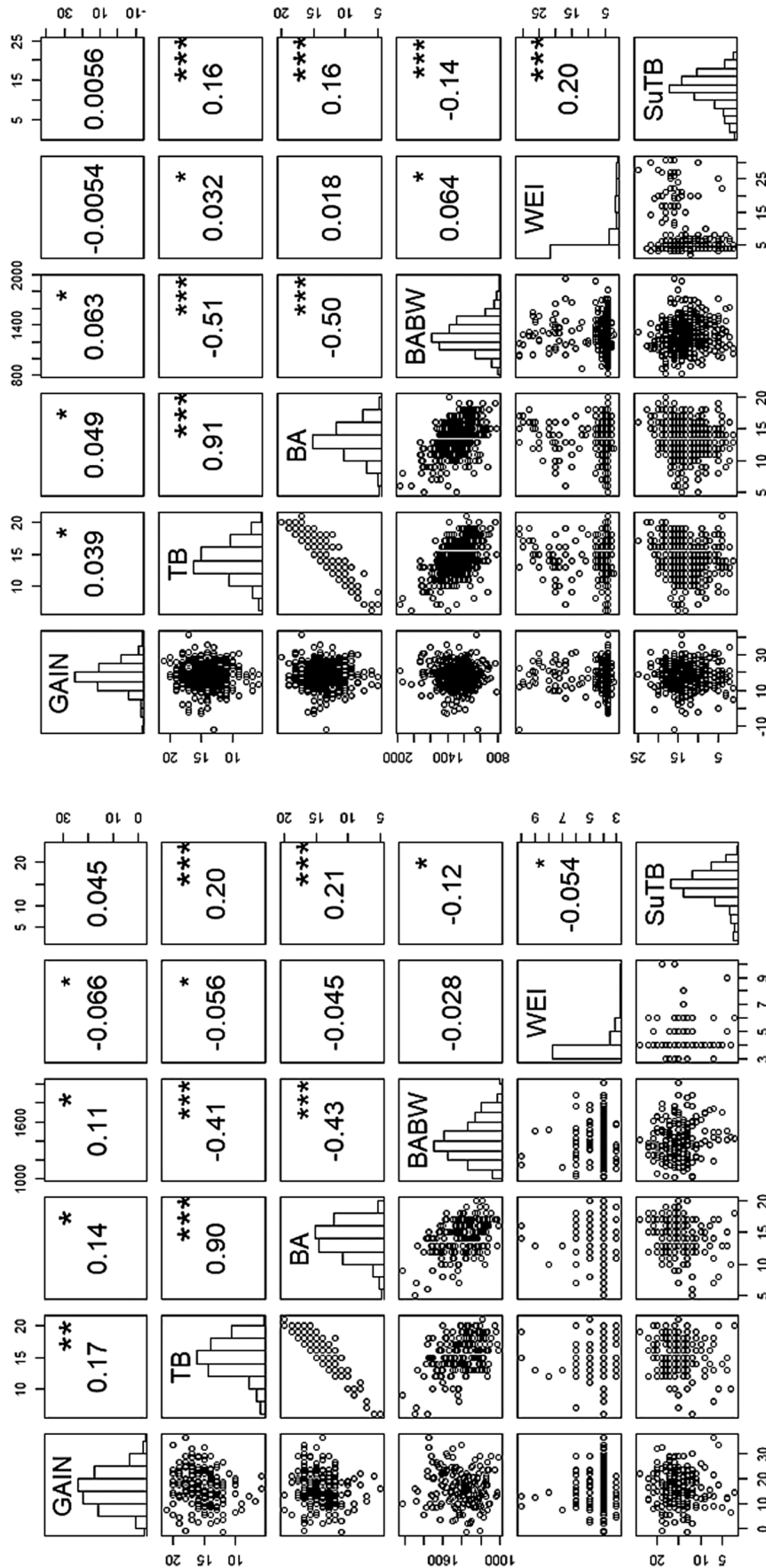
Figure 1. Scatterplot matrices depicting the empirical distributions and marginal associations between reproductive performance traits in sows (left panel) and in gilts (right panel). For each panel, histograms are shown along the main diagonal, whereas bivariate scatterplots are shown on the lower triangle and estimated Pearson correlation coefficients are presented on the upper triangle. Asterisks indicate that the coefficient is significantly different from zero (***P-value < 0.0001, **P-value < 0.01, *P-value < 0.05). GAIN = female weight gain during late gestation; TB = total number born in a litter; BA = number born alive in a litter; BABW = born alive average body weight; WEI = wean-to-estrous interval; SuTB = total number born in the subsequent gestation.

Figure 2. (A) Undirected graph of reproductive performance traits in sows detected by the inductive causation algorithm implemented with 80% highest posterior density intervals. (B) Plausible structures within the equivalence class defined by traits connected in Panel (A). Links without arrowheads represent associations between traits; links with arrowheads represent causal effects from the trait on the arrow tail to the trait on the arrowhead. GAIN = female weight gain during late gestation; TB = total number born in a litter; BA = number born alive in a litter; BABW = born alive average body weight; WEI = wean-to-estrous interval; SuTB = total number born in the subsequent gestation.
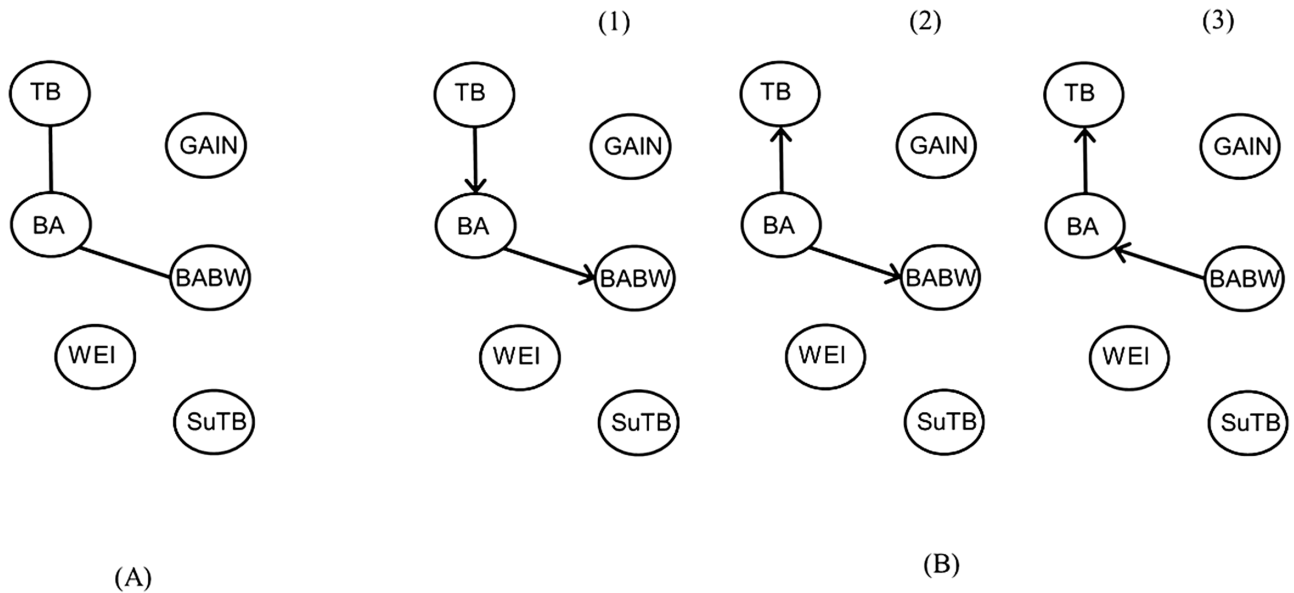

Figure 3. (A) Partially oriented graph of reproductive performance traits in gilts detected by the inductive causation algorithm implemented with 80% highest posterior density intervals. (B) Fully oriented graph obtained after incorporating additional temporal information to (A). Links without arrowheads represent associations between traits; links with arrowheads represent causal effects from the trait on the arrow tail to the trait on the arrowhead. GAIN = female weight gain during late gestation; TB = total number born in a litter; BA = number born alive in a litter; BABW = born alive average body weight; WEI = wean-to-estrous interval; SuTB = total number born in the subsequent gestation.
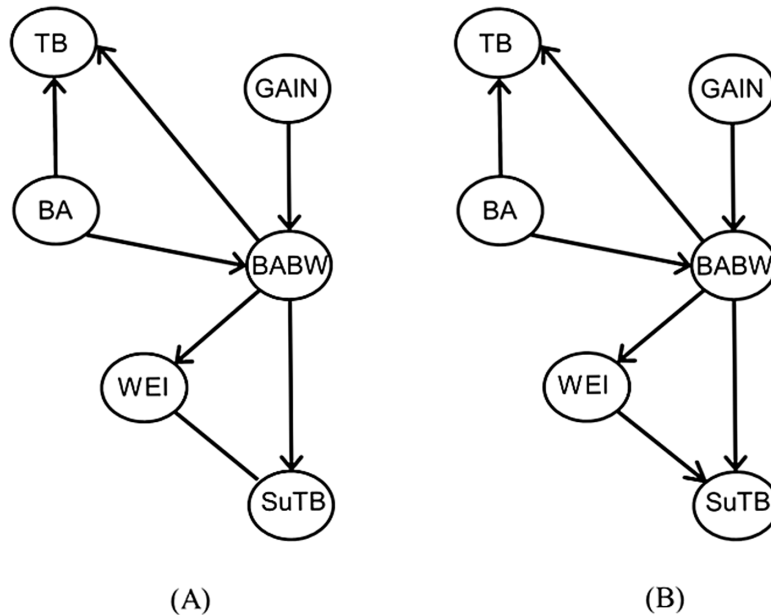
BABW), which in turn affected TB (i.e., BABW → TB). Also detected were effects of BA on TB (i.e., BA → TB) and on BABW (i.e., BA → BABW). Notably, the link connecting BA and BABW (i.e., BA → BABW) prevented TB to function as an unshielded collider between BABW and BA. Further, effects of BABW were detected on subsequent

reproductive performance of gilts, as characterized by WEI and SuTB (i.e., BABW → WEI and BABW → SuTB, respectively). Finally, a link between WEI and SuTB was detected in gilts, though the IC algorithm was inconclusive about its directionality. We used temporal information to tentatively orient the link as WEI → SuTB and relied on DIC to further
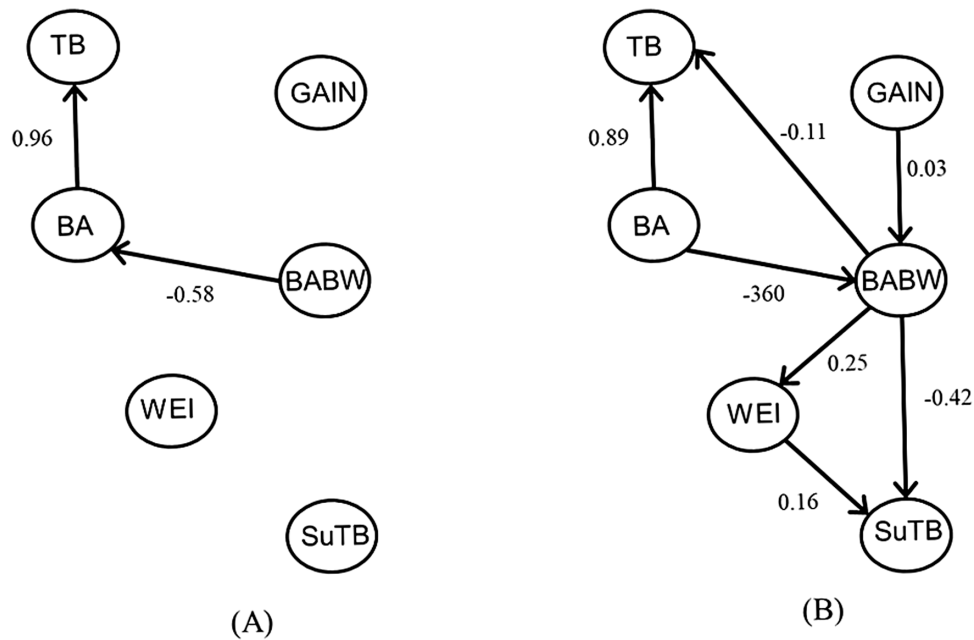
Figure 4. Links and posterior means of structural coefficients between reproductive performance traits in sows (A) and in gilts (B) learned using a mixed-models adapted inductive causation algorithm implemented with 80% highest posterior density intervals. Refer to Table 2 for further details. GAIN = female weight gain during late gestation; TB = total number born in a litter; BA = number born alive in a litter; BABW = born alive average body weight; WEI = wean-to-estrous interval; SuTB = total number born in the subsequent gestation.

evaluate this model choice. The difference in DIC between a learned network presuming the selected direction (i.e., WEI → SuTB) versus the same network with a reversed link (i.e., WEI ← SuTB) was smaller than 1 point (i.e., DIC values were 11974.86 and 11974.09, respectively). Such small DIC difference suggested that there was no information available in the data to select one network over the other. As a result, we relied solely on qualitative information (e.g., temporal arrangement of the traits) to inform directionality of this link (Fig. 3B).

SEM-Based Inference

Figure 4 shows the causal network structures selected for final inference on the potentially causal relationships between reproductive performance traits of (Fig. 4A) sows and (Fig. 4B) gilts. Table 2 shows posterior summaries of the corresponding structural coefficients representing direct effects between traits.

For sows, BABW was found to have a direct effect on BA (i.e., BABW → BA) by which every 100-g increase in average BABW resulted in an estimated decrease in BA of about [posterior mean (95% HPD)] = 0.58 (0.41, 0.77) piglets. Subsequently, every additional piglet BA increased the TB in a sow litter (i.e., BA → TB) by approximately 0.96 (0.89, 1.02) piglets.

For gilts, BA had a direct effect on both TB and BABW. Specifically, every unit increase in BA

resulted in an increase in TB of 0.89 (0.85, 0.94) piglets and in an estimated decrease of about 360 g (240, 480) in BABW. Moreover, in gilts, BABW also had a direct effect on TB and on SuTB. In particular, a l00-g increase in average BABW resulted in an estimated decrease of 0.11 (0.05, 0.17) in TB and of 0.42 (0.20, 0.65) in SuTB. Finally, WEI had a direct effect on SuTB, whereby a 1-d increase in WEI resulted in an estimated increase in SuTB of 0.16 (0.09, 0.24) piglets per litter. Additional direct effects yielded by the network learning process are presented in Table 2 but are not discussed further, as the 95% HPD interval for the corresponding structural coefficients overlapped with the null value zero.

For completeness of network interpretation, we also report indirect effects, which under linearity assumptions can be computed as the product of the corresponding structural coefficients, as described by Shipley (2002). For example, for sows, the indirect, BA-mediated effect of BABW on TB (i.e., BABW → BA → TB) was estimated as the product of the corresponding direct effects, namely $\lambda_{TB, BA} \times \lambda_{BA, BABW}$, the posterior density of which had a mean of −0.56 TB per 100-g increase in BABW with 95% HPD = (−0.74, −0.39). Indirect effects for gilts are presented in Table 3 and can be interpreted in a similar manner. For gilts, most indirect effects had 95% HPD intervals that overlapped with zero, except for the BABW-mediated effects of BA on TB (i.e., BA → BABW → TB) and of BA on SuTB (i.e., BA → BABW → SuTB) (Table 3).

Table 2. Posterior means and 95% highest posterior density (HPD) intervals of structural coefficients from the final structural equation models selected for inference separately for sows and for gilts based on the inductive causation algorithm

			Sows		Gilts	
Structural coefficient	From[1]	To[1]	Posterior mean	95% HPD interval	Posterior mean	95% HPD interval
$\lambda_{BA, BABW}$, unit/100 g	BABW	BA	−0.58	−0.77, −0.41	–	–
$\lambda_{BABW, BA}$, g/unit	BA	BABW	–	–	−360	−480, −240
$\lambda_{BABW, GAIN}$, g/kg	GAIN	BABW	–	–	0.03	−0.02, 0.09
$\lambda_{TB, BA}$, unit/unit	BA	TB	0.96	0.89, 1.02	0.89	0.85, 0.94
$\lambda_{TB, BABW}$, unit/100 g	BABW	TB	–	–	−0.11	−0.17, −0.05
$\lambda_{WEI, BABW}$, day/100 g	BABW	WEI	–	–	0.25	−0.04, 0.55
$\lambda_{SuTB, BABW}$, unit/100 g	BABW	SuTB	–	–	−0.42	−0.65, −0.20
$\lambda_{SuTB, WEI}$, unit/day	WEI	SuTB	–	–	0.16	0.09, 0.24

[1]GAIN = female weight gain during late gestation; TB = total number born in a litter; BA = number born alive in a litter; BABW = born alive average body weight; WEI = wean-to-estrous interval; SuTB = total number born in the subsequent gestation.

Table 3. Posterior means and 95% highest posterior density (HPD) intervals of indirect and total causal effects from the final structural equation models selected for inference separately for gilts based on the inductive causation algorithm

		Gilts	
Causal effect	Formulaic expression	Posterior mean	95% HPD interval
Indirect effects[1]			
GAIN → BABW → TB[2], unit/kg	$\lambda_{TB, BABW} \times \lambda_{BABW, GAIN}$	−0.004	−0.011, 0.003
GAIN → BABW → WEI, day/kg	$\lambda_{WEI, BABW} \times \lambda_{BABW, GAIN}$	0.007	−0.008, 0.029
GAIN → BABW → SuTB, unit/kg	$\lambda_{SuTB, BABW} \times \lambda_{BABW, GAIN}$	−0.01	−0.04, 0.01
GAIN → BABW → WEI → SuTB, unit/kg	$\lambda_{SuTB, WEI} \times \lambda_{WEI, BABW} \times \lambda_{BABW, GAIN}$	0.001	−0.001, 0.005
BA → BABW → TB, unit/unit	$\lambda_{TB, BABW} \times \lambda_{BABW, BA}$	0.04	0.02, 0.07
BA → BABW → SuTB, unit/unit	$\lambda_{SuTB, BABW} \times \lambda_{BABW, BA}$	0.16	0.06, 0.25
BA → BABW →WEI→ TB, unit/unit	$\lambda_{SuTB, WEI} \times \lambda_{WEI, BABW} \times \lambda_{BABW, BA}$	−0.015	−0.036, 0.004
BABW → WEI → SuTB, unit/100 g	$\lambda_{SuTB, WEI} \times \lambda_{WEI, BABW}$	0.41	−0.10, 0.95
Total effects[3]			
GAIN → SuTB, unit/kg	$(\lambda_{SuTB, BABW} \times \lambda_{BABW, GAIN}) + (\lambda_{SuTB, WEI} \times \lambda_{WEI, BABW} \times \lambda_{BABW, GAIN})$	−0.01	−0.04, 0.01
BA → TB, unit/unit	$(\lambda_{TB, BABW} \times \lambda_{BABW, BA}) + \lambda_{TB, BA}$	0.94	0.89, 0.98
BA → SuTB, unit/unit	$(\lambda_{SuTB, BABW} \times \lambda_{BABW, BA}) + (\lambda_{SuTB, WEI} \times \lambda_{WEI, BABW} \times \lambda_{BABW, BA})$	0.14	0.05, 0.24
BABW → SuTB, unit/100 g	$(\lambda_{SuTB, WEI} \times \lambda_{WEI, BABW}) + \lambda_{SuTB, WEI}$	0.57	0.05, 1.15

[1]Indirect effects are computed as the product of the corresponding direct effects represented by structural coefficients.

[2]GAIN = female weight gain during late gestation; TB = total number born in a litter; BA = number born alive in a litter; BABW = born alive average body weight; WEI = wean-to-estrous interval; SuTB = total number born in the subsequent gestation.

[3]Total effects are computed as the sum of the direct effect and all indirect effects.

Finally, Table 3 also shows total effects, reported as the sum of the direct effect and all indirect effects connecting 2 traits, as described by Shipley (2002). For example, the total effect of BA on TB is obtained as $(\lambda_{TB, BABW} \times \lambda_{BABW, BA}) + \lambda_{TB, BA}$ and had a posterior mean of 0.94 TB per additional BA with 95% HPD = (0.89, 0.98).

Assessment of Network Stability

The stability of the learned network was assessed using a Jackknife resampling approach modified to leave-one-block-out at each resampling iteration. Figure 5 shows results of network stability for (Fig. 5A) sows and (Fig. 5B) gilts at the level of individual links and expressed as the percent of resampled datasets (i.e., 97 for sows, 222 for gilts) for which each link was present in the learned network structure.

For sows, the link between TB and BA was recovered in 100% of the resampled datasets, whereas the link between BA and BABW appeared in 92% of the cases. The reproductive traits GAIN, WEI, and SuTB remained unconnected to any other nodes in all cases. Notably, no link directionality was recovered from any of the resampled datasets. Overall,
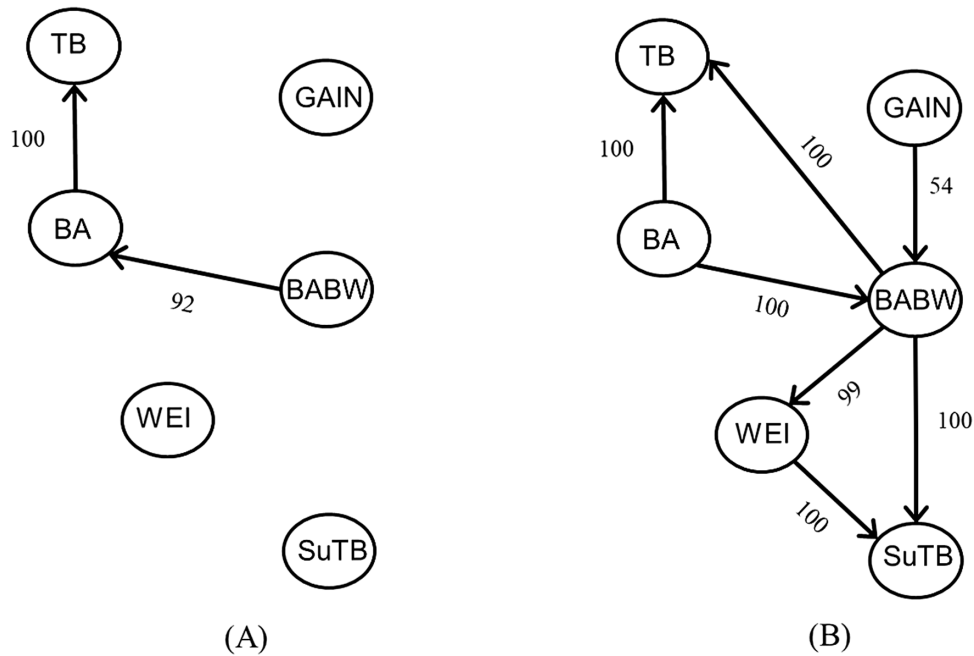
Figure 5. Stability analysis of the learned network of reproductive performance traits for sows (A) and gilts (B) using a leave-one-block-out Jackknife resampling approach. Values (%) indicate the percentage of resampled datasets for which each link was present in the learned network structure. GAIN = female weight gain during late gestation; TB = total number born in a litter; BA = number born alive in a litter; BABW = born alive average body weight; WEI = wean-to-estrous interval; SuTB = total number born in the subsequent gestation.

Figure 6. Network structures learned from 5 subsets (labeled panels A–E) created from the gilt dataset by random sampling without replacement, to mimic the sow dataset in size and structure. GAIN = female weight gain during late gestation; TB = total number born in a litter; BA = number born alive in a litter; BABW = born alive average body weight; WEI = wean-to-estrous interval; SuTB = total number born in the subsequent gestation.
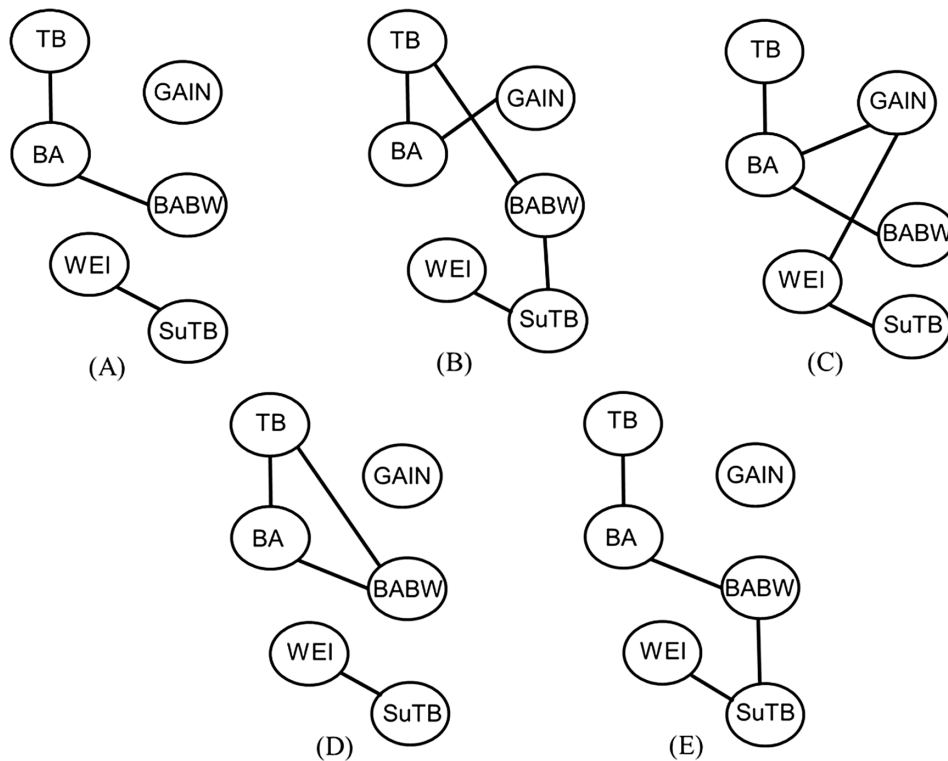
the network structure learned for sows was considered stable, though not so the directionality of the links.

For gilts, most links connecting reproductive traits showed substantial stability as their presence ranged from 99% to 100% of the resampled datasets (Fig. 5B). A notable exception was the link connecting GAIN and BABW, which was present in only 54% of the cases. This link showed the least

stability in the gilt network, as removal of a single block negated its presence in almost half (101 out of 222) of the resampled datasets. Recall that the link between GAIN and BABW was deemed pivotal for assessing directionality of effects within the gilt network; specifically, this link informed an unshielded collider with BA (i.e., GAIN → BABW ← BA), while negating any unshielded colliders between GAIN and other non-adjacent traits, namely TB, WEI, and SuTB. Similar to sows, the general network structure of reproductive traits in gilts was deemed stable, though the evidence for directionality of effects was considered weak.

Relative Power Differences in Network Learning

Figure 6 shows the network structures learned from each of the 5 gilt data subsets that were sampled to mimic the sow dataset in size and structure. First, we note that no unshielded colliders were detected in any of the gilt data subsets; as a result, it was not possible to learn directionality of individual links from any dataset smaller than the complete gilt dataset. This suggests a relative sample-size-based power differential between parity groups for learning directionality within the network; admittedly, thought, results on directionality were weak for both gilts and sows. Second, the network structure learned from each of the 5 gilt data subsets showed a number of links ranging from 3 to 5 (Fig. 6), in contrast to only 2 links learned from the complete sow data and 7 links learned from the complete gilt dataset. The intermediate number of links detected from the gilt data subsets suggests non-power-based differences in network structure, presumably of a biological basis, to partially explain the parity difference in links recovered. In particular, all 5 gilt data subsets consistently identified a specific link that was not apparent from the sow dataset, namely the link between WEI and SuTB.

DISCUSSION

In this study, we investigated potentially causal biological relationships among reproductive performance traits in experimental data from high-performing gilts and sows. To accomplish this, we used a network approach implemented with SEMs and the IC algorithm to search the structure space of interrelationships between reproductive traits. We followed recent methodological developments that extended networks to a mixed-model framework (Gianola and Sorensen, 2004; Valente et al., 2010) in order to accommodate the inherently hierarchical nature of experimental data. The analytic approach

of hierarchical network modeling formalizes integration from a systems perspective, thus enabling more comprehensive insight into the complex mechanisms that underlie animal production.

Consistent with the distinct reproductive physiology of sows and gilts (Da Silva et al., 2016; 2017), our results indicate disparate network connectivity across parity groups. Gilts showed a densely interconnected network between all 6 reproductive performance traits considered in this study. Notably, direct effects connected reproductive events starting at first gestation (i.e., GAIN) through first farrowing (i.e., BABW, TB, and BA) and into the subsequent reproductive cycle (i.e., WEI, SuTB). By contrast, sows showed a sparse network depicting only connections within the immediate farrowing event (i.e., BABW, BA, and TB), but without any temporal connections with earlier or later stages of the reproductive lifecycle (i.e., GAIN, WEI, and SuTB were completely disconnected from the rest of the traits). This differential network connectivity between parity groups may be partially explained by the fact that sows are mature adults, whereas gilts are immature animals still growing after the first farrowing event and into the first lactation (Kraeling and Webel, 2015). As such, gilts are subjected to competing requirements for growth and reproduction, which can be expected to impact subsequent reproductive performance. Indeed, the high level of network connectivity observed in gilts suggests potential propagating ripple effects across the physiological network and productive lifecycle. This is consistent with the current state of the literature, which indicates that performance of parity one sows (which are referred to as gilts in this study) is a critical contributing factor to subsequent reproductive performance and ultimately, sow longevity in the herd (Mabry et al., 1996; Rozeboom et al., 1996). Indeed, our results show direct effects and total effects connecting stages of the gilt lifecycle (e.g., BABW and SuTB), suggesting longer-term impact of early reproductive events.

In contrast, the sparser network recovered in sows suggests a mitigated potential for long-term propagation of intervention effects once females have reached maturity and adult size. One may interpret this result as an opportunity for compounding long-term beneficial effects in response to early managerial interventions. As such, special attention and tailored management of gilts during the first farrowing and lactation seems warranted. Undoubtedly, modern swine females across the parity spectrum require continuous updating of nutrient requirements to maximize productive efficiency and are highly responsive to management

practices and technologies (Boyd et al., 2002; Kraeling and Webel, 2015). This is specially the case for young females from modern maternal lines, as they seem to be particularly sensitive to finely tuned managerial practices because of a lower appetite and exceptional lean growth potential despite large competing nutritional demands from gestation (Bortolozzo et al., 2009). This is consistent with current recommendations for tailored management of dietary nutrient density and feeding intake of gilts during first lactation, as this may enhance their long-term reproductive performance and longevity in the production system (Kraeling and Webel, 2015). For example, tailored feeding strategist such as segregated phase feeding is often recommended (Kraeling and Webel, 2015) to ensure feed intake is matched with nutrient requirements of younger gilts still undergoing growth.

In addition, the influence of season and environmental conditions on reproductive performance of swine females is well documented (Kraeling and Webel, 2015). Gilts seem to be most vulnerable to seasonal infertility in response to extreme temperature and disruptions in photoperiod, with reported consequences of delayed estrus after weaning and disrupted estrus behavior, among others (Britt et al., 1983; Wettemann and Bazer, 1985; Tummaruk et al., 2004; Auvigne et al., 2010), as consistent with results from this study. This is relevant to our discussion because data collection for this study was conducted during summer months. Due to enhanced sensitivity, gilts might also be expected to respond to tailored modulations of the ambient environment (e.g., cooling devices, group size, equipment, and facilities) and to dietary management of nutrient density (McGlone et al., 1988; 2004; Kraeling and Webel, 2015).

As we continue to ponder connectivity of the reproductive network in sows and gilts, it is worth mentioning that all links recovered from the sow dataset and most of those from the gilt dataset were validated as inferentially stable using Jackknife resampling. Moreover, a power assessment acknowledged a potential biological basis for differences in network connectivity. Admittedly, differences in sample size between the parity groups may underlie and partially explain some of the observed differences, as the gilt dataset was almost twice as large as the sow dataset. Yet, the power assessment recovered more links (i.e., ranging from 3 to 5; Fig. 6) in every one of the 5 gilt data subsets compared to the 2 links recovered from the complete sow data, suggesting additional non-power-related (presumably biological) reasons for the observed network discrepancies between parity groups. Worth highlighting

is the link connecting WEI and SuTB, both indicators of reproductive performance in the subsequent gestation. This link was consistently recovered from all 5 gilt data subsets as well as from the complete gilt dataset, but was not apparent in sows. This may be partially explained by the fact that, in the post-weaning period, gilts are typically less effective in the recovery of mobilized tissue and body condition score compared to sows, and tend to redirect energy and nutrients towards ensuring mature size growth over reproductive functions (Rempel et al., 2015), thus delaying estrous and rebreeding. It is then not unexpected that subsequent reproductive performance of gilts is more sensitive to WEI than that of sows. For this reason, maximizing nutrient intake during lactation seems to be especially important in gilts.

The network-type SEM approach implemented in this study raises the issue of statistical power as an important point in need of serious consideration for proper implementation of these methods in the context of animal agriculture. Recall that the swine datasets used in this study might be considered substantial in size for a designed experiment (i.e., > 3,800 observations from 640 females). Yet, this experiment was arguably not designed for network analysis and the dataset may still not be big enough to have adequate power for learning network structure or assessing network differences. In particular, inference on directionality of links seems to be specially sensitive to power. For illustration, consider the sow dataset (the smallest of the 2 datasets), consisting of a total of 1,200 observations collected from 200 females (i.e., 6 traits × 200 sows), for which the IC algorithm failed to assign direction to any of the links. Further, Jackknife resampling failed to identify direction for any link in sows, such that link orientation for final inference in this parity group was based on relative model fit to the observed data. Even with the complete gilt dataset, which consisted of a total of 2,640 observations collected from 440 females (i.e., 6 traits × 440 gilts), directionality of links turned out to be the weakest of our results. Specifically, recall that directionality of the gilt network hinged on the link recovered between GAIN and BABW, which in turn oriented most other links in the network by detecting (or negating) the role of BABW as an unshielded collider with other nodes. Yet, the link between GAIn and BABW was not inferentially stable, as it was detected in only 54% of the Jackknife resampling folds. Overall, it appears that even larger datasets with informative structures will be needed to ensure sufficient statistical power for network learning in order to reliably explore how traits affect each other in an integrated system.

In pork production systems, an important aspect of profitability is the number of piglets produced per sow per year (Kraeling and Webel, 2015). To this end, swine breeding programs have emphasized selection for increased litter sizes (Johnson et al., 1999) over the past few decades. Larger litter sizes have been associated with lower birth weight (Town et al., 2004), which in turn has implications for pre-weaning mortality rate and further piglet development (Milligan et al., 2002). This is likely due to compromised placental development in the crowded uterus (Père et al., 1997) and associated competition for nutrients and space throughout gestation (Geisert and Schmitt, 2002). Indeed, piglets of lower average birth weight are weaker and less likely to survive, thus posing economic and welfare concerns. Our findings are conceptually consistent with this understanding, particularly regarding the interrelationships between piglet birth weight and survivability. Specifically, BABW as a node played a key role in both sow and gilt networks; further, the structural coefficients connecting BABW and BA showed negative signs and thus supported inverse relationships between the traits in both parity groups.

Also, both parity groups showed a connection between litter size and piglet survivability, as depicted by the recovery of a link connecting BA and TB. Our next discussion emphasizes presence, rather than direction, of this link, as results on directionality were considered weak in this study, as discussed earlier. Piglet mortality at birth seems to be a multifactorial problem, with contributing factors including litter size and parity, among others (Vanderhaeghe et al., 2013). While not a formal comparison, we observed seemingly disparate magnitudes of the association between BA and TB in gilts and in sows. Specifically, in sows, every unit increase in BA resulted in a larger litter size by approximately 1 unit, as the 95% HPD of $\lambda_{TB,BA} = (0.89, 1.02)$ contained the value 1. For gilts, a piglet increase in BA translated into a proportionally smaller increase in litter size, as the corresponding 95% HPD (i.e., 0.85, 0.94) was below the value 1. This could be partially explained by physiological differences in uterine capacity between the parity groups (Ford et al., 2002), and the resulting timing of embryonic mortality due to uterine overcrowding (Foxcroft et al., 2009). Uterine capacity is critical for the development and survivability of the pig conceptus (Chen and Dziuk, 1993) due to its influence on placental growth and thus, supply of nutrients to the conceptus (Ford et al., 2002). Swine females, in general, but particularly gilts, typically have limited uterine capacity relative to their ovulation rate

(Da Silva et al., 2016). In gilts, this precipitates uterine crowding and conceptus losses in earlier stages of gestation (Da Silva et al., 2017). Embryos that die before day 30 to day 35 of gestation are often reabsorbed, but any fetuses that are lost after day 30 to day 35 are accounted for at farrowing either as mummies or stillborn piglets (Foxcroft et al., 2009). Therefore, our results can be explained by gilts having higher embryonic loss in the early gestation period (Da Silva et al., 2017), thus unobservable at birth; whereas sows with higher uterine capacity may be able to maintain fetal development longer into the pregnancy, thereby resulting in proportionally higher losses at later stages of gestation, which are then observable at birth.

Identification of parity differences in the magnitude of effects along the reproductive network is arguably of interest to inform tailored management and efficient decision making of each category of animals. In this study, each parity group was analyzed separately such that it is not possible to conduct formal tests for parity differences on the structural coefficients connecting, say, BA and TB. Yet, separate analyses were inevitable in this case because of the standard assumption of SEMs that structural coefficients be homogeneous across the population (Gianola and Sorensen, 2004), thereby curtailing formal testing, even if a joint analysis of sows and gilts were conducted. Methodological developments are warranted to explicitly allow specification of sources of heterogeneity on structural coefficients in SEM. Additional methodological extensions relevant to SEMs in animal agriculture include heterogeneity of variance parameters, as a way to stabilize the variance of traits with skewed distributions, such as WEI in this study. Here, we considered a variance-stabilizing transformation on WEI, though this was not pursued because it is unclear what the implications of doing so might be for simultaneous modeling of WEI as a response and as a predictor, as well as for interpretation of indirect and total effects given linearity assumptions of SEM. The inferential implications of SEM assumptions of normality and homogeneous variances for all traits require further study.

Specification of the network structure is critical to SEM. The IC algorithm is one of many strategies available to conduct a data-driven search for network structure and directionality compatible with the joint probability distribution of the data (Spirtes et al., 1993). In a rather informal follow-up step to the IC algorithm, a researcher can incorporate additional information to assist

with remaining undirected links and thus differentiate between models within an equivalence class. Admittedly, such incorporation of information is subject-matter-based and rather ad hoc in nature, and thus, does not guarantee causality. For example, in this study, the direction of the link connecting WEI and SuTB in gilts was not resolved by the IC algorithm. To fully orient the gilt network, we incorporated temporal information and set WEI → SuTB, as later events cannot have an effect on earlier events. Another type of information that can be used to assist in orienting left-over undirected links in the context of structured data is an indicator of model fit. Here, we used DIC (Spiegelhalter et al., 2002) to select between SEM specifications compatible with the undirected graph yielded by the IC algorithm for the sow dataset, as shown in Fig. 2B. These 3 SEM specifications correspond to the same equivalence class defined at the residual level by the mixed-models-adapted IC algorithm (Valente et al., 2010). In this adaptation of the IC algorithm, the residual-level equivalence class is defined after fitting random effects to account for correlation patterns in the data due to experimental design or other structural components of the data, such as genetic relationships (Inoue et al., 2016). By contrast, recall that the DIC is an indicator of model fit computed based on the deviance statistic and as such, uses the joint likelihood of the observed data (as opposed to that of residuals). That is, the mixed-models-adapted IC algorithm searches for network structure on the residual (co)variance matrix R^* [rather than on the (co)variance matrix of the observed data $var(y) = ZB^*Z' + R^*$, for $B^* = (I - \Lambda)^{-1}B(I - \Lambda)^{-1}$], thus yielding a class of equivalent models defined at the residual level (Valente et al., 2010). Differences in goodness of data fit between otherwise residual-level equivalent models should then not be surprising, provided there is structure of distribution of random effects; in fact, DIC differences are to be anticipated in such case. Indeed, discrepancies in the selection of SEM structure from DIC relative to the mixed-models-adapted IC algorithm were also reported by Inoue et al. (2016). Specifically for this study, data architecture proved useful in the implementation of DIC to differentiate between competing sow networks (Fig. 2A), as indicated by DIC differences of 20 points or more between competing SEM specifications.

In using the IC algorithm, it is important to assess stability of the learned network structures before proceeding further with inference. Following Peñagaricano et al. (2015), we adapted Jackknife resampling to network learning and implemented the sampling strategy so as to leave-one-*block*-out at a time instead of the more traditional leave-one-*observation*-out. This was intended as a trade-off for computational efficiency in the assessment of network stability. This approach is consistent with Dórea et al., (2018), who used a machine-learning strategy to leave-one-*trial*-out of the dataset at a time when validating feed intake predictions in lactating dairy cows. So adapted, Jackknife resampling might be considered a validation strategy in a broader scope of inference (Bello and Renter, 2018) across the population for which the body weight blocks used in this study [or trials used by Dórea et al. (2018)] might be considered a representative, if not random, sample.

Admittedly, in and of themselves, the statistical methodology that underlies SEM does not guarantee causal claims. As an example, we refer the reader to the inferential weaknesses described for this study in the learning of directionality of direct effects. In designed experiments, the conclusion of a causal effect of a treatment of interest is supported by randomization, which is considered the gold standard for causal inference (Bello et al., 2018). It is often overlooked, though, that such randomization-based causal claims are restricted to the effect of treatment on a response variable of interest; yet, randomization does not support causality of one response variable on another, as is of interest for the type of causal phenotypic networks that motivated this study. That is, even in designed experiments, causal relationships between response variables of interest may be confounded by other variables (either observed or unobserved) or even by correlations induced by the design structure (i.e., within-block correlations). It is for this reason that causal identification requires that non-trivial causal assumptions be made (Pearl, 2009), even in the context of designed experiments. Briefly, these assumptions comprise the Markov condition, the assumption of faithfulness or stability, and causal sufficiency. The latter assumption, causal sufficiency, is probably the most delicate one because it implies that any confounders in the system are known and either have been measured or can be controlled for by other measured variables. Importantly, these causal assumptions are not directly testable from data and yet are fundamental for further inference, as explained by Bello et al. (2018). Despite these limitations, we strongly believe that the framework of causal inference offers promising practical advantages for scientific progress (Bello et al., 2018). For example, insight gained from causal inference can help subject-matter scientists identify and refine research hypotheses that, ideally, could then be tested in tailored randomized experiments conducted in vivo or in vitro. From a

study design standpoint, causal inference can further help elucidate what set of variables should be measured and which others might be redundant, thereby enhancing efficiency in the allocation and use of research funding. More broadly, causal inference undeniably contributes to the growing body of scientific evidence on which science advances.

CONCLUSION

This study provides insight into potentially causal biological networks of interconnected reproductive performance traits in high-producing sows and gilts, based on SEMs and the IC algorithm adapted to mixed models. Evidence suggests distinct networks for these parity groups, consistent with differences in their reproductive physiology, thereby substantiating tailored reproductive management specific for each category of animals. Further investigation of network connectivity, directionality, and sources of heterogeneity is warranted to improve integrated understanding and efficient management of swine production systems.

SUPPLEMENTARY DATA

Supplementary data are available at *Journal of Animal Science* online.

LITERATURE CITED

Auvigne, V., P. Leneveu, C. Jehannin, O. Peltoniemi, and E. Sallé. 2010. Seasonal infertility in sows: a five year field study to analyze the relative roles of heat stress and photoperiod. Theriogenology 74:60–66. doi:10.1016/j.theriogenology.2009.12.019

Bello, N. M., V. C. Ferreira, D. Gianola, and G. J. M. Rosa. 2018. Conceptual framework for investigating causal effects from observational data in livestock. J. Anim. Sci. 96:4045–4062. doi:10.1093/jas/sky277

Bello, N. M., and D. G. Renter. 2018. Invited review: reproducible research from noisy data: revisiting key statistical principles for the animal sciences. J. Dairy Sci. 101:5679–5701. doi:10.3168/jds.2017-13978

Bortolozzo, F. P., M. L. Bernardi, R. Kummer, and I. Wentz. 2009. Growth, body state and breeding performance in gilts and primiparous sows. Soc. Reprod. Fertil. Suppl. 66:281–291. PMID: 19848294.

Boyd, D. R., G. C. Castro and R. A. Cabrera. 2002. Nutrition and management of the sow to maximize lifetime productivity. Adv. Pork Prod. 13:47–59.

Britt, J. H., V. E. Szarek, and D. G. Levis. 1983. Characterization of summer infertility of sows in large confinement units. Theriogenology 20:133–140. doi:10.1016/0093-691X(83)90032-8

Chen, Z. Y., and P. J. Dziuk. 1993. Influence of initial length of uterus per embryo and gestation stage on prenatal survival, development, and sex ratio in the pig. J. Anim. Sci. 71:1895–1901. doi:10.2527/1993.7171895x

Cowles, M. K., and B. P. Carlin. 1996. Markov chain Monte Carlo convergence diagnostics: a comparative review. J. Am. Stat. Assoc. 91:883–904. doi:10.1080/01621459.1996.10476956

Da Silva, C. L. A., B. F. A. Laurenssen, E. F. Knol, B. Kemp, and N. M. Soede. 2017. Validation of transrectal ultrasonography for assessment of corpora lutea characteristics in pregnant sows and its relationship with litter characteristics at birth. Transl. Anim. Sci. 1:507–517. doi:10.2527/tas2017.0057

Da Silva, C. L., H. van den Brand, B. F. Laurenssen, M. L. Broekhuijse, E. F. Knol, B. Kemp, and N. M. Soede. 2016. Relationships between ovulation rate and embryonic and placental characteristics in multiparous sows at 35 days of pregnancy. Animal 10:1192–1199. doi:10.1017/S175173111600015X

de los Campos, G., D. Gianola, P. Boettcher, and P. Moroni. 2006. A structural equation model for describing relationships between somatic cell score and milk yield in dairy goats. J. Anim. Sci. 84:2934–2941. doi:10.2527/jas.2006-016

de Maturana, E. L., X. L. Wu, D. Gianola, K. A. Weigel, and G. J. Rosa. 2009. Exploring biological relationships between calving traits in primiparous cattle with a Bayesian recursive model. Genetics 181:277–287. doi:10.1534/genetics.108.094888

Dórea, J. R. R., G. J. M. Rosa, K. A. Weld, and L. E. Armentano. 2018. Mining data from milk infrared spectroscopy to improve feed intake predictions in lactating dairy cows. J. Dairy Sci. 101:5878–5889. doi:10.3168/jds.2017-13997

Ford, S. P., K. A. Vonnahme, and M. E. Wilson. 2002. Uterine capacity in the pig reflects a combination of uterine environment and conceptus genotype effects. J. Anim. Sci. 80(E. Suppl. 1):E66–E73. doi:10.2527/animalsci2002.0021881200800ES10010x

Foxcroft, G. R., W. T. Dixon, M. K. Dyck, S. Novak, J. C. Harding, and F. C. Almeida. 2009. Prenatal programming of postnatal development in the pig. Soc. Reprod. Fertil. Suppl. 66:213–231. PMID: 19848290.

Geisert, R. D., and R. A. M. Schmitt. 2002. Early embryonic survival in the pig: can it be improved? J. Anim. Sci. 80:E54–E65. doi:10.2527/animalsci2002.0021881200800ES10009x

Gelman, A. 2006. Prior distributions for variance parameters in hierarchical models. Bayesian Anal. 1:515–533. doi:10.1214/06-BA117A

Gianola, D., and D. Sorensen. 2004. Quantitative genetic models for describing simultaneous and recursive relationships between phenotypes. Genetics 167:1407–1424. doi:10.1534/genetics.103.025734

Gonçalves, M. A., K. M. Gourley, S. S. Dritz, M. D. Tokach, N. M. Bello, J. M. DeRouchey, J. C. Woodworth, and R. D. Goodband. 2016. Effects of amino acids and energy intake during late gestation of high-performing gilts and sows on litter and reproductive performance under commercial conditions. J. Anim. Sci. 94:1993–2003. doi:10.2527/jas.2015-0087

Haavelmo, T. 1943. The statistical implications of a system of simultaneous equations. Econometrica 11:1–12. doi:10.2307/1905714

Henderson, C. R., and R. L. Quaas. 1976. Multiple trait evaluation using relatives records. J. Anim. Sci. 43:1188–1197. doi:10.2527/jas1976.4361188x

Inoue, K., B. D. Valente, N. Shoji, T. Honda, K. Oyama, and G. J. Rosa. 2016. Inferring phenotypic causal structures

among meat quality traits and the application of a structural equation model in Japanese black cattle. J. Anim. Sci. 94:4133–4142. doi:10.2527/jas.2016-0554

Johnson, R. K., M. K. Nielsen, and D. S. Casey. 1999. Responses in ovulation rate, embryonal survival, and litter traits in swine to 14 generations of selection to increase litter size. J. Anim. Sci. 77:541–557. doi:10.2527/1999.773541x

Kraeling, R. R., and S. K. Webel. 2015. Current strategies for reproductive management of gilts and sows in North America. J. Anim. Sci. Biotechnol. 6:3. doi:10.1186/2049-1891-6-3

Mabry, J., M. S. Culbertson, and D. Reeves. 1996. Effects of lactation length on weaning-to-first-service interval, first-service farrowing rate, and subsequent litter size. Swine Health Prod. 4:185–188. PMID: 11191874.

McGlone, J. J., W. F. Stansbury, and L. F. Tribble. 1988. Management of lactating sows during heat stress: effects of water drip, snout coolers, floor type and a high energy-density diet. J. Anim. Sci. 66:885–891. PMID: 3378948.

McGlone, J. J., E. H. von Borell, J. Deen, A. K. Johnson, D. G. Levis, M. Meunier-Salaon, J. Morrow, D. Reeves, J. L. Salak-Johnson, and P. L. Sundberg. 2004. Reviews: compilation of the scientific literature comparing housing systems for gestating sows and gilts using measures of physiology, behavior, performance, and health. Prof. Anim. Sci. 20:105–117. doi:10.15232/S1080-7446(15)31285–7

Milligan, B. N., D. Fraser, and D. L. Kramer. 2002. Within-litter birth weight variation in the domestic pig and its relation to pre-weaning survival, weight gain, and variation in weaning weights. Livest. Prod. Sci. 76:181–191. doi:10.1016/S0301-6226(02)00012-X

Pearl, J. 2009. Causality: models, reasoning, and inference. 2nd ed. Cambridge University Press, New York.

Peñagaricano, F., B. D. Valente, J. P. Steibel, R. O. Bates, C. W. Ernst, H. Khatib, and G. J. Rosa. 2015. Exploring causal networks underlying fat deposition and muscularity in pigs through the integration of phenotypic, genotypic and transcriptomic data. BMC Syst. Biol. 9:58. doi:10.1186/s12918-015-0207-6

Père, M. C., J. Y. Dourmad, and M. Etienne. 1997. Effect of number of pig embryos in the uterus on their survival and development and on maternal metabolism. J. Anim. Sci. 75:1337–1342. PMID: 9159282.

Raftery, A., and S. Lewis. 1992. How many iterations in the Gibbs sampler? Bayesian Stat. 4:763–773. doi:10.1.1.41.6474

R Development Core Team. 2017. R: a language and environment for statistical computing. R Foundation for Statistical Computing, Vienna, Austria.

Rempel, L. A., J. L. Vallet, C. A. Lents, and D. J. Nonneman. 2015. Measurements of body composition during late gestation and lactation in first and second parity sows and its relationship to piglet production and post-weaning reproductive performance. Livest. Sci. 178:289–295. doi:10.1016/j.livsci.2015.05.036

Robinson, G. K. 1991. That BLUP is a good thing: the estimation of random effects. Stat. Sci. 6:15–32. doi:10.1214/ss/1177011926

Rozeboom, D. W., J. E. Pettigrew, R. L. Moser, S. G. Cornelius, and S. M. el Kandelgy. 1996. Influence of gilt age and body composition at first breeding on sow reproductive performance and longevity. J. Anim. Sci. 74:138–150. PMID: 8778092.

Shipley, B. 2002. Cause and correlation in biology: a user's guide to path analysis, structural equations and causal inference. 1st ed. Cambridge University Press, New York.

Sorensen, D. A., S. Andersen, D. Gianola, and I. Korsgaard. 1995. Bayesian inference in threshold model using Gibbs sampling. Genet. Sel. Evol. 27:229–249. doi:10.1051/gse:19950303

Spiegelhalter, D. J., N. G. Best, B. P. Carlin, and A. Van Der Linde. 2002. Bayesian measures of model complexity and fit. J. Royal Stat. Soc. 64(Series B):583–639. doi:10.1111/1467–9868.00353

Spirtes, P., Glymour, C., and Scheines, R. 1993. Causation, prediction, and search. Springer-Verlag, New York.

Town, S. C., C. T. Putman, N. J. Turchinsky, W. T. Dixon, and G. R. Foxcroft. 2004. Number of conceptuses in utero affects porcine fetal muscle development. Reproduction 128:443–454. doi:10.1530/rep.1.00069

Tummaruk, P., W. Tantasuparuk, M. Techakumphu, and A. Kunavongkrit. 2004. Effect of season and outdoor climate on litter size at birth in purebred Landrace and Yorkshire sows in Thailand. J. Vet. Med. Sci. 66:477–482. PMID: 15187355.

Valente, B. D., and G. M. J. Rosa. 2013. Mixed Effects Structural Equation Models and Phenotypic Causal Networks. In: Gondro, C. et al., editors. Genome-wide association studies and genomic prediction. Totowa, NJ: Humana Press. p. 449–464.

Valente, B. D., G. J. Rosa, G. de Los Campos, D. Gianola, and M. A. Silva. 2010. Searching for recursive causal structures in multivariate quantitative genetics mixed models. Genetics 185:633–644. doi:10.1534/genetics.109.112979

Valente, B. D., G. J. Rosa, M. A. Silva, R. B. Teixeira, and R. A. Torres. 2011. Searching for phenotypic causal networks involving complex traits: an application to European quail. Genet. Sel. Evol. 43:37. doi:10.1186/1297-9686-43-37

Vanderhaeghe, C., J. Dewulf, A. de Kruif, and D. Maes. 2013. Non-infectious factors associated with stillbirth in pigs: a review. Anim. Reprod. Sci. 139:76–88. doi:10.1016/j.anireprosci.2013.03.007

Van Vleck, L. D., and K. M. Edlin. 1984. Multiple trait evaluation of bulls for calving ease. J. Dairy Sci. 67:3025–3033. doi:10.3168/jds.S0022-0302(84)81668–9

Varona, L., and D. Sorensen. 2014. Joint analysis of binomial and continuous traits with a recursive model: a case study using mortality and litter size of pigs. Genetics 196:643–651. doi:10.1534/genetics.113.159475

Verma, T., and J. Pearl. 1991. Equivalence and synthesis of causal models Proceedings of the Sixth Annual Conference on Uncertainty in Artificial Intelligence. Elsevier Science Inc, New York. p. 255–270.

Wettemann, R. P., and F. W. Bazer. 1985. Influence of environmental temperature on prolificacy of pigs. J. Reprod. Fertil. Suppl. 33:199–208. PMID: 3910825.

Wright, S. 1934. An analysis of variability in number of digits in an inbred strain of guinea pigs. Genetics 19:506–536. PMID: 17246735.

Wu, X. L., B. Heringstad, Y. M. Chang, G. de Los Campos, and D. Gianola. 2007. Inferring relationships between somatic cell score and milk yield using simultaneous and recursive models. J. Dairy Sci. 90:3508–3521. doi:10.3168/jds.2006-762